Materials Today Bio 26 (2024) 101072

Contents lists available at ScienceDirect

Materials Today Bio

journal homepage: www.journals.elsevier.com/materials-today-bio

A personalized osteoarthritic joint-on-a-chip as a screening platform for biological treatments

Dalila Petta [a,b,1], Daniele D'Arrigo [a,b,c,1], Shima Salehi [d], Giuseppe Talò [d], Lorenzo Bonetti [e], Marco Vanoni [c], Luca Deabate [b], Luigi De Nardo [e], Gabriele Dubini [e], Christian Candrian [b,f], Matteo Moretti [a,b,d,f], Silvia Lopa [d,*], Chiara Arrigoni [a,b,f]

[a] Regenerative Medicine Technologies Lab, Laboratories for Translational Research, Ente Ospedaliero Cantonale, Via Chiesa, 5, 6500, Bellinzona, Switzerland
[b] Service of Orthopaedics and Traumatology, Department of Surgery, Ente Ospedaliero Cantonale, Via Tesserete 46, 6900, Lugano, Switzerland
[c] ISBE-SYSBIO Centre of Systems Biology, Milan, Italy at Department of Biotechnology and Biosciences, Università Degli Studi di Milano Bicocca, Piazza Della Scienza 2, 20126, Milan, Italy
[d] Cell and Tissue Engineering Laboratory, IRCCS Istituto Ortopedico Galeazzi, Via Belgioioso 173, 20157, Milan, Italy
[e] Department of Chemistry, Materials and Chemical Engineering G.Natta, Politecnico di Milano, Piazza Leonardo da Vinci 32, 20133, Milan, Italy
[f] Euler Institute, Biomedical Sciences Faculty, Università Della Svizzera Italiana (USI), Via Buffi 13, 6900, Lugano, Switzerland

ARTICLE INFO

Keywords:
Joint-on-a-chip
Osteoarthritis
Microfluidics
Chondrogenic matrix
Orthobiologics
Cartilage
Inflammation
Mesenchymal stem cells

ABSTRACT

Osteoarthritis (OA) is a highly disabling pathology, characterized by synovial inflammation and cartilage degeneration. Orthobiologics have shown promising results in OA treatment thanks to their ability to influence articular cells and modulate the inflammatory OA environment. Considering their complex mechanism of action, the development of reliable and relevant joint models appears as crucial to select the best orthobiologics for each patient.

The aim of this study was to establish a microfluidic OA model to test therapies in a personalized human setting. The joint-on-a-chip model included cartilage and synovial compartments, containing hydrogel-embedded chondrocytes and synovial fibroblasts, separated by a channel for synovial fluid. For the cartilage compartment, a Hyaluronic Acid-based matrix was selected to preserve chondrocyte phenotype. Adding OA synovial fluid induced the production of inflammatory cytokines and degradative enzymes, generating an OA microenvironment. Personalized models were generated using patient-matched cells and synovial fluid to test the efficacy of mesenchymal stem cells on OA signatures. The patient-specific models allowed monitoring changes induced by cell injection, highlighting different individual responses to the treatment. Altogether, these results support the use of this joint-on-a-chip model as a prognostic tool to screen the patient-specific efficacy of orthobiologics.

1. Introduction

Osteoarthritis (OA) is the most prevalent form of arthritis and the leading cause of disability in adults, imposing a high socioeconomic burden on the healthcare system [1]. The most evident clinical outcome of OA is progressive articular cartilage degeneration. However, associated synovial tissue inflammation and subchondral bone alterations characterize OA as a whole joint disorder [2], in which inflammation is deeply involved [3]. Since pathological mechanisms underlying this multifactorial disease are not thoroughly understood, current treatments concentrate predominantly on symptom suppression through anti-inflammatory drugs. More recently, approaches consisting in the intraarticular injection of orthobiologics, including platelet-rich plasma (PRP), bone marrow concentrate, adipose and bone marrow mesenchymal stem cells or their secretome have been proposed to modulate the degradative microenvironment by promoting joint homeostasis and counteracting cartilage degeneration [4,5]. Although orthobiologics have demonstrated promising outcomes in functional improvement and symptom relief, their mechanism of action needs to be investigated to improve treatment efficacy. In this scenario, developing relevant models to study OA pathogenesis and compare innovative therapeutics is paramount. Besides being characterized by ethical issues, animal models cannot always be considered fully reliable, due to differences in

* Corresponding author. IRCCS Istituto Ortopedico Galeazzi, Via Belgioioso 173, 20161, Milan, Italy.
E-mail address: silvia.lopa@grupposandonato.com (S. Lopa).
[1] contributed equally to this work.

https://doi.org/10.1016/j.mtbio.2024.101072
Received 29 November 2023; Received in revised form 3 April 2024; Accepted 25 April 2024
Available online 6 May 2024

Abbreviation list:

OA	Osteoarthritis
SynFlu	Synovial Fluid
HA	Hyaluronic Acid
HA-MA	Methacrylated Hyaluronic Acid
HA-PEGDA	Hyaluronic Acid crosslinked with Polyethylene Glycol Diacrylate (PEGDA)
Col	Collagen
Col-MA	Methacrylated Collagen
BMSCs	Bone Marrow derived Mesenchymal Stem Cells
ASCs	Adipose derived Mesenchymal Stem Cells
ROI	Regions of Interest
FI	Fluorescence Intensity

pathological mechanisms and drug responses, particularly for inflammatory diseases [6]. On the other hand, currently available *in vitro* models fail to recapitulate the complexity of articular joints since they generally focus only on cartilage, neglecting the contribution of other joint elements [7]. Thus, complex *in vitro* models, mimicking the joint microenvironment, represent a possible solution to accelerate the development of new OA treatments.

Microfluidics is a powerful technique for 3D *in vitro* modeling of human diseases and for evaluating candidate therapeutics. Microfluidic models enable recapitulating cell-matrix and cell-cell interactions within compartmentalized 3D microenvironments, requiring minimal amounts of cells and reagents [8]. Although many *in vitro* joint models have been developed, ranging from 2D co-cultures to 3D multi-tissue microfluidic devices [9], only few of them have been reliably exploited to study the pathogenesis of OA and test potential therapies. Recently, a joint-on-a-chip model including synovium and cartilage was developed by our group to study monocyte extravasation in osteoarthritic conditions and evaluate potential inhibitors of this process [10], while in another recent study, a cartilage-on-a-chip model was used to investigate the role of mechanical compression and test candidate drugs [11].

Herein, we designed a microfluidic model recapitulating different joint elements, including the synovial membrane, the articular cartilage, and the joint cavity, filled with synovial fluid. To mimic the synovial compartment, we included synovial fibroblasts in a fibrin matrix, based on previous models optimized by our group. As chondrocyte behavior is highly influenced by the extracellular environment [12], to mimic the cartilage matrix, which is a heterogeneous mix of collagen, proteoglycans, and hyaluronic acid (HA) [12,13], we evaluated different hydrogels based on collagen and HA. We then added OA synovial fluid in the system and verified the onset of OA hallmarks. Finally, we built patient-specific models and used them for a proof-of-concept screening of orthobiologics, comparing the effects of mesenchymal stem cells derived from bone marrow (BMSCs) and adipose tissue (ASCs).

2. Materials and methods

2.1. Model design and fabrication

Aiming at generating a joint-on-a-chip model, we firstly designed a customized microfluidic device (Fig. 1A and B), starting from a CAD design of the mold (Supplementary Fig. 1). The central channel was designed to host the synovial fluid (SynFlu), while the two flanking hydrogel compartments, delimited by trapezoidal posts to prevent hydrogel leakage during injection, were designed to host articular chondrocytes and synovial fibroblasts. Two external channels were dedicated to the culture medium. The mold was then 3D printed using a digital light processing (DLP) printer with a resolution of 27 μm in the x and y axes and 25 μm in the z-axis (Asiga MAX X UV) using Detax Freeprint model 2.0 Resin photopolymer, followed by post-curing under UV light of the mold. The printed mold showed a good fidelity with the original CAD design, resulting in a relative error between the dimensions below 2.5 % (Supplementary Fig. 1). The polydimethylsiloxane (PDMS), prepared in a 10:1 ratio as per the manufacturer's instructions, was poured into the mold and cured in an oven at 65 °C for 3 h. Subsequently, the PDMS chip was extracted from the mold and autoclaved and dried at 65 °C for at least 12 h. Finally, the devices were plasma-bonded with a plasma cleaner (Harrick-plasma, US) to glass slides (Ø 35 mm) and incubated overnight at 65 °C.

2.2. Biological samples and ethics statement

The human-derived specimen sampling was conducted under the guidelines, regulations, and procedures of the Ente Ospedaliero Cantonale (Bellinzona, Switzerland) and approved by the local IRB (Approval n. 2020-00029 from Comitato Etico Cantonale). The biological samples used in the study are represented by waste surgical pieces, harvested from patients who signed an informed consent. All the patients (4 males, 3 females) were subjected to knee replacement surgery and presented OA Kellgren Lawrence grade 3 to 4, evaluated from radiological images. The age of the patients ranged between 41 and 85 years. Details of the biological materials harvested, patient of origin, and experiments in which they were used are reported in Table S1.

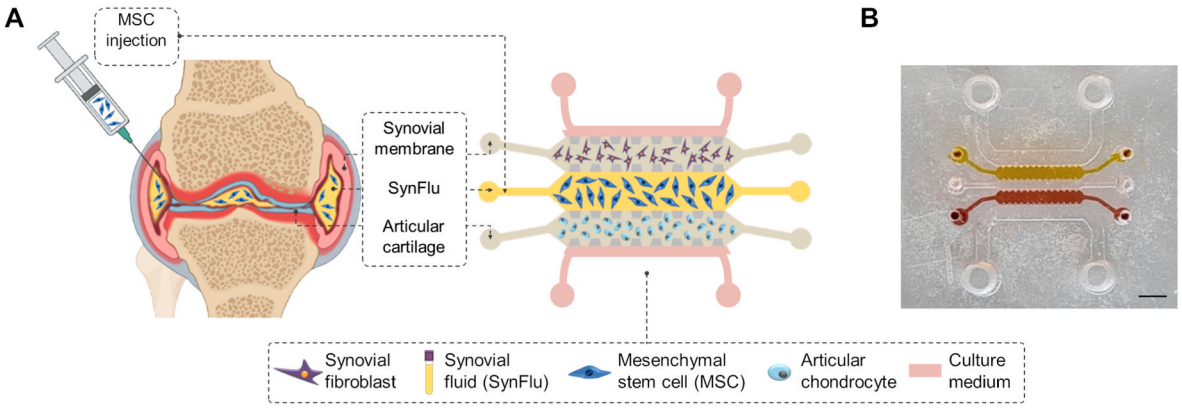

Fig. 1. Design and development of the microfluidic device. **(A)** Schematic of an OA knee joint and application of an injective therapy based on mesenchymal stem cells, illustrating how each component is reproduced in the chip. **(B)** Micrograph of the device with channels dedicated to synovial and chondral compartments highlighted in yellow and red, respectively. Scale bar: 2 mm. (For interpretation of the references to colour in this figure legend, the reader is referred to the Web version of this article.)

2.3. Preparation of primary cells and synovial fluid

For the harvesting of cartilage, femoral condyles and tibial plateau of patients were rinsed in PBS under a laminar flow hood and superficial layers were sliced with a sterile surgical blade. Cartilage and synovial membrane were minced into small pieces. Subsequently, the synovial membrane was digested with 2.5 mg/mL Collagenase type I (Worthington Biochemical Corporation) in complete culture medium (DMEM-CM) consisting of Dulbecco's modified Eagle medium (DMEM) High-Glucose, 10 % fetal bovine serum (FBS), 2 mM L-glutamine, 100 U/mL penicillin, 100 μg/mL streptomycin, 10 mM 4-(2-hydroxyethyl)-1-piperazineethanesulfonic acid (HEPES), 1 mM sodium pyruvate (all from Gibco, ThermoFisher Scientific) for 3 h in an orbital shaker (110 rpm) at 37 °C. Cartilage was treated with 0.15 % Collagenase type II in DMEM-CM for 22 h in the same conditions. After enzymatic digestion, Collagenase was inactivated by adding the same volume of DMEM-CM, and tissue debris were removed using a 100 μm cell strainer. Synovial fibroblasts and chondrocytes were plated at 5000 cells/cm^2 and cultured in DMEM-CM and DMEM-CM added with 1 ng/mL TGF-β1 and 5 ng/mL basic-FGF (bFGF), respectively [14]. After expansion, cells were frozen for subsequent experiments.

Adipose tissue was digested with 0.075 % Collagenase type I in MSC-CM (Minimum Essential Medium Eagle-Alpha Modification (α-MEM), 10 % FBS, 100 U/mL penicillin, 100 μg/mL streptomycin, 10 mM HEPES) for 30 min at 37 °C. After blocking the Collagenase and removing tissue debris, ASCs were plated at 5000 cells/cm^2 in MSC-CM added with 5 ng/mL bFGF. The bone marrow was centrifuged at 510*g* for 10 min at room temperature (RT). Then, cells were suspended in MSC-CM added with 5 ng/mL bFGF and plated. After one week, adherent BMSCs were washed with PBS to remove red blood cells. ASCs and BMSCs were cultured until passage 2 and then frozen. Synovial fluid from OA donors (OA-SynFlu) was harvested from patients undergoing knee replacement before surgical operation through a syringe puncture of the joint capsule. OA-SynFlu was centrifuged immediately after harvesting at 3000*g* for 5 min at 4 °C to remove cells and debris. The supernatant was collected, aliquoted and stored at −80 °C.

For non-patient-specific experiments, we created pools of chondrocytes, synovial fibroblasts, BMSCs, and ASCs. Pools of cells were generated by mixing the same number of cells from each donor, plating and culturing the pooled cells until passage 3. Similarly, we created pools of OA-SynFlu by mixing SynFlu from multiple OA donors.

2.4. Hydrogel preparation

Different hydrogels were tested as 3D matrix for the cartilage compartment (Table 1). Cell-laden fibrin gels were prepared by suspending chondrocytes or synovial fibroblasts in 4 U/mL thrombin diluted in culture medium and mixing the solution with the same volume of 40 mg/mL fibrinogen (Sigma-Aldrich), to obtain a final fibrin concentration of 20 mg/mL. Cell-free fibrin gels were also prepared for rheological testing. As alternative matrices for mimicking cartilage tissue, we evaluated different combinations of photocrosslinkable Hyaluronic acid (HA) and Collagen (Col) derivatives, namely HA-MA (degree of methacrylation 45–65 %) and Col-MA (degree of methacrylation 20 %) (Advanced BioMatrix). Briefly, lyophilized Col-MA was reconstituted at 8 mg/mL concentration by adding 20 mM acetic acid and incubating overnight under stirring at 4 °C. HA-MA was employed at a final 15 mg/mL concentration. Col-MA/HA-MA (MIX) hydrogels were obtained by mixing the two polymers at selected ratios (1:2, Col-MA 3 mg/mL and HA-MA 6 mg/mL; 1:6, Col-MA 2 mg/mL and HA-MA 12 mg/mL) and triggering the triple helix formation of Col-MA by pH neutralization and temperature (37 °C). The final photo-crosslinking was triggered by light exposure (UV light, 365 nm, 30 mW/cm^2), using Lithium phenyl-2,4,6-trimethylbenzoylphosphinate (LAP) (Sigma-Aldrich) as photoinitiator. Additionally, HA-PEGDA (Advanced BioMatrix) was employed. The gelation of HA-PEGDA was obtained by mixing the two components in a ratio of 1:4 and incubating the material at 37 °C for 30 min. To embed cells in the hydrogels, chondrocytes were suspended in the pre-gels at 1.5x10^6 cells/mL, then crosslinked with pH neutralization and incubation at 37 °C or applying UV crosslinking as described above.

Table 1
Hydrogels produced and evaluated for the cartilage compartment. Polymer concentration and crosslinking strategy are reported for each hydrogel.

Hydrogel	Gel concentration (mg/mL)			Crosslinking Strategy
	Fibrin	Collagen	HA	
Fibrin	20	–	–	Enzymatic (Thrombin 4 U/mL)
HA-MA	–	–	15	Photocrosslinking
HA-PEGDA	–	–	6	Chemical
MIX Col-MA/HA-MA (1:2)	–	3	6	Physical + Photocrosslinking
MIX Col-MA/HA-MA (1:6)	–	2	12	Physical + Photocrosslinking

2.5. Rheology

The viscoelastic properties of the hydrogels were assessed with a rotational rheometer (MCR 302, Anton Paar) equipped with a parallel plate geometry (Ø 25 mm, working gap 0.2 mm). Flow curves (0.1–1000 s^{-1} shear rate γ range) were carried out at 25 °C on each pre-gel formulation to assess their injectability. Additionally, strain sweep tests were performed by applying an oscillatory strain (γ) in the 0.01–100 % strain range at 1 Hz frequency (ν) to determine the linear viscoelastic region of each formulation and, where applicable, the effects of physical (temperature-mediated) and chemical (UV-mediated) crosslinking. Strain sweep tests were conducted at 25 °C and 37 °C after UV-curing for photocrosslinkable gels. Where applicable, time sweep tests ($\gamma = 0.5$ %, $\nu = 1$ Hz, T = 37 °C) were performed within 30 min to determine the cross-linking kinetics. The parameters of the rheological tests are reported in Table S2.

2.6. Live/dead assay

Cell viability was assessed by Live/Dead assay (ThermoFisher Scientific), following manufacturer's instructions. Briefly, the staining solution containing 10 μM Calcein AM and 1 μM Ethidium Homodimer-1 in serum-free DMEM was injected in the medium channels of the chips and samples were incubated for 30 min at 37 °C. After incubation, chondrocytes and synovial fibroblasts in the respective compartments (cell density 1.5x10^6 cells/mL) were imaged with a fluorescence microscope (Eclipse Ti, Nikon) equipped with a CCD camera (Nikon DS-QiMc). For each sample, three different areas were acquired. Chondrocyte and synovial fibroblast viability was quantified by counting red (dead) and green (viable) cells with the software Image J.

2.7. Mimicking an OA environment in the model

Chondrocyte and synovial fibroblast pools were seeded in the microfluidic chip at a final density of 1.5x10^6 cells/mL. This cell density was previously optimized to prevent hydrogel degradation and cell sprouting from the gel. Cell-laden gels were prepared as described above and injected in the respective channels (6 μL of cell suspension, containing 10^4 cells, in each channel). Chips were incubated in a humidified chamber at 37 °C for hydrogel polymerization. We injected 5 μL of pooled OA-SynFlu or serum-free medium into the central channel. The serum-free medium, named culture medium throughout the text, consisted of DMEM High-Glucose supplemented with 2 mM L-glutamine, 100 U/mL penicillin, 100 μg/mL streptomycin, 10 mM HEPES (all from Gibco, ThermoFisher), 1 % ITS+ (10 μg/mL insulin, 5.5 μg/mL human

transferrin and 6.7 ng/mL sodium selenite; Corning) and 1.25 mg/mL of Human Serum Albumin (Sigma-Aldrich). Afterwards, we added 100 μL of the serum-free medium in the external channels. Finally, the chips were transferred to a 6-well plate and cultured for 1, 4, or 10 days, refreshing the medium or the SynFlu only on day 4. To evaluate the generation of an inflammatory microenvironment, we assessed cell viability, lineage-specific phenotype, and the secretion of pro- and anti-inflammatory cytokines and degradative enzymes, as described in the following paragraphs.

2.8. Patient-specific OA joint-on-a-chip models

Chondrocytes and synovial fibroblasts isolated from the same OA patient were seeded in the chips, as previously described. After cell seeding, we added patient-matched OA-SynFlu in the central channel and serum-free medium in the external channels. The devices were cultured for 10 days (37 °C, 5 % CO_2). On day 4, fresh medium was added to the outer channels, and ASCs or BMSCs were injected into the central channel. Briefly, pooled BMSCs and ASCs were suspended in the patient-derived OA-SynFlu at a concentration of $1x10^6$ cells/mL and injected in the central channel of the device, simulating an intraarticular injection of allogeneic MSCs. In the control group, we injected only OA-SynFlu. We cultured the chips until day 10, then performed immunofluorescence analyses and the quantification of cytokine production.

2.9. Senescence-associated β-Galactosidase assay

Senescence-Associated β-Galactosidase (SA-β-Gal) which is known to be expressed by senescent cells was detected using Senescence Detection Kit (BioVision) according to the provider's protocol. Briefly, X-gal solution was prepared by dissolving 20 mg of X-gal in 1 mL of dimethyl sulfoxide (DMSO) to create a stock solution. For sample preparation, chip channels were initially washed with PBS and subsequently the cells were fixed using the Fixative Solution included in the kit for 10–15 min at room temperature. During cell fixation, the Staining Solution Mix was prepared using 470 μL of Staining Solution, 5 μL of Staining supplement and 25 μL of 20 mg/mL X-gal in DMSO. After fixing and washing the cells with PBS, the prepared mix was added to medium channels and samples were incubated at 37 °C overnight. Finally, cells were observed under a microscope and the images were taken using a bright field camera with 80 μm z-stacks. The cells with blue signal were considered positive and counted as senescent cells.

2.10. Immunofluorescence staining

We performed immunofluorescence analysis to check the phenotype of articular chondrocytes and synovial fibroblasts and to assess the expression of MMPs and pro-inflammatory cytokines (TNFα and IL8). For MMPs and cytokine staining, we first blocked protein secretion by incubating the chips with 5 μg/mL Brefeldin-A (ab193369, Abcam) in serum-free medium for 5 h at 37 °C. Then, we fixed the samples with 4 % paraformaldehyde for 10 min at room temperature and blocked the non-specific binding site with 5 % bovine serum albumin (BSA, Sigma-Aldrich). Then, we added the following primary antibodies diluted in BSA 0.1 %: anti-Collagen-I (ab34710, 2 μg/mL, rabbit, Abcam), anti-Collagen-II (MA5-12789, 2 μg/mL, mouse, ThermoFisher Scientific), anti-Aggrecan (MA3-16888, 4 μg/mL, mouse, ThermoFisher Scientific), anti-Lubricin (PA3-118, 5 μg/mL, rabbit, Invitrogen), anti-IL8 (sc-376750, 2 μg/mL, mouse, Santa Cruz Biotechnology), anti-TNFα (sc-133192, 2 μg/mL, mouse, Santa Cruz Biotechnology), anti-MMP1 (ab52631, 6.6 μg/mL, rabbit, Abcam), and anti-MMP13 (sc-515284, 1 μg/mL, mouse, Santa Cruz Biotechnology). After 1 h at 37 °C, the primary antibodies were washed away, and the secondary antibody was added and incubated for 1 h at 37 °C. We used anti-mouse Alexafluor 488 and anti-rabbit Alexafluor 568 secondary antibodies (both at 2 μg/mL in PBS, Thermofisher Scientific). Finally, the nuclei were stained with NucBlue™ Fixed Cell ReadyProbes™ Reagent (DAPI) (R37606, ThermoFisher Scientific) for 20 min at RT.

2.11. Image analysis

Z-stacks were acquired with a Leica SP8 confocal microscope and analyzed by ImageJ for signal quantification. A customized macro was developed to split channels, generate a Z projection with max intensity for each channel and merge the projections.

A threshold was applied for each channel, and the function "Analyze Particles" was applied to exclude particles smaller than 10 μm^2 and isolate all the signal spots. The spots were then converted to a mask and applied to the original non-thresholded image channels to define the Regions of Interest (ROIs). To evaluate the signal intensity only in the previously extracted ROIs, the command "Measure" of the ROI Manager was used.

To obtain a "weighted fluorescence intensity (FI)" for each marker, the following formula was applied:

$$Weighted\ FI = \frac{\sum (a_n \times FI_n)}{\sum a_n}$$

Where a_n was the Area of a specific ROI and FI_n was the mean Fluorescence Intensity of the same ROI. The sum of products between Area and Mean Fluorescence Intensity of each ROI detected in a single image was then divided by the sum of the Areas of all the ROIs detected in the same image. This elaboration allowed obtaining a parameter relative to the fluorescence intensity weighted for the corresponding area. This parameter was then normalized by the total area positive for each marker to compare different images, which might include a different number of cells.

2.12. Cytokine quantification

The concentration of soluble cytokines (IL8, IFNγ, IL10, IL13, IL1α, IL1β, IL4, IL6, TNFα) was determined by Quantibody® Human Inflammation Array Q1 (RayBiotech, Norcross, GA, USA) in the cell culture medium of the chips and in the synovial fluids, according to the manufacturer's instructions. Culture media were diluted 1:2 and synovial fluids 1:40 to fit the standard curves. The mean cytokine concentration was reported as ng/mL. Additionally, values for each cytokine measured in the patient-specific chips in the presence of BMSCs and ASCs were normalized to the control condition (Ctrl, no BMSCs/ASCs) set at 1.

2.13. Statistical analysis

Independent triplicates were prepared and analyzed for each experimental condition. Prism GraphPad Version 8.0.2 was used for the statistical analysis. A Two-Way ANOVA followed by Dunnet's multiple comparison test was applied to compare multiple groups at multiple time points. T-test or One-Way ANOVA followed by Dunnet's multiple comparison test were applied to compare two or multiple groups at the same time point, respectively. Statistical significance was defined as $p < 0.05$.

3. Results

3.1. Synovial compartment

Synovial fibroblasts embedded in fibrin within the chip synovial compartment, showed cell viability values higher than 80 % at all timepoints, reaching 91 % on day 10 (Fig. 2A). We then checked the phenotype of synovial fibroblasts by assessing the expression of Collagen-I and Lubricin. Collagen-I expression was detected after 4 days and resulted slightly decreased at day 10 (Fig. 2B). Differently, Lubricin was detected after 4 days and increased during culture (Fig. 2C).

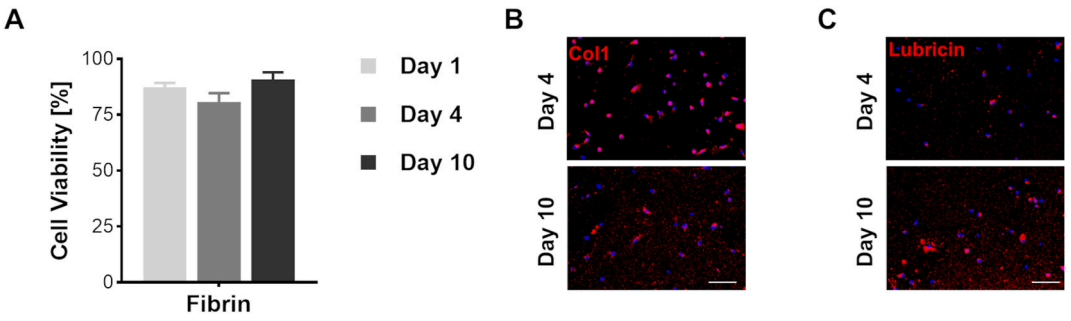

Fig. 2. Characterization of the synovial compartment. **(A)** Viability of synovial fibroblasts in fibrin hydrogel after 1, 4, and 10 days of culture (n = 3). **(B,C)** Expression of typical markers of synovial fibroblasts: Collagen-I (Col1) and Lubricin (both in red) in fibrin hydrogels. Nuclei are counterstained with DAPI (blue). Scale bars: 100 μm. (For interpretation of the references to colour in this figure legend, the reader is referred to the Web version of this article.)

3.2. Cartilage compartment

To select the hydrogel matrix for the cartilage compartment, we firstly verified if the pre-gel rheological properties were compatible with the chip injection, performing shear rate sweep tests. The flow curves (Fig. 3A) displayed a shear-thinning behavior for all the tested formulations, thus assuring the feasibility of hydrogel injection in the device. Regarding the kinetics of chemical and physical crosslinking for the hydrogel formulations (Fig. 3B), both MIX 1:2 and MIX 1:6 displayed a rapid increase in the viscoelastic parameters, plateauing after 1 min, whilst HA-PEGDA reached the gelation point after 6 min and a complete polymerization within 30 min. Fibrin showed a significant increase in G' within the first 10 min, hence all the different formulations showed a gelation time compatible with gel injection in the chip.

For all the tested specimens, G′ was almost constant at low shear strains, indicating a linear viscoelastic regime, consistently higher than G″, confirming a gel-like behavior (Fig. 3C) [15]. Except HA-PEGDA, for which yielding was not reached within the strain range tested, all the other specimens entered a yielding region for higher strain values, undergoing a decrease in their structural resistance (G′ decrease). G′ in MIX 1:2 was similar to MIX 1:6 and higher than fibrin, which displayed G′ values of ~300 Pa in the linear viscoelastic range. HA-PEGDA and HA-MA presented the lowest viscoelastic moduli, with G′ values of ~100 Pa at low strain. Interestingly, for double-crosslinked gels G' values after physical crosslinking alone (129 Pa and 34.5 Pa at 0.1 % strain for MIX 1:2 and MIX 1:6 respectively) were significantly lower than after UV irradiation (390 Pa and 478 Pa at 0.1 % strain for MIX 1:2 and MIX 1:6 respectively, Fig. S2). Overall, all the selected formulations were compatible with both our joint-on-a-chip device in terms of viscoelastic properties (injectability, gelation time, and elasticity).

As shown in Fig. 3D, cell viability significantly decreased for all the tested gels at day 10 compared to day 1. Among HA- and Col-based materials, chondrocytes embedded in HA-PEGDA showed the highest cell viability at day 10 (72 %). The viability of chondrocytes cultured in the MIX 1:6 hydrogel was significantly lower than fibrin at days 1 and 10 ($p < 0.01$ and $p < 0.001$, respectively), indicating a low cytocompatibility of this formulation.

Chondrocyte morphology was different among different gels, with cells in fibrin showing a spindle-shaped morphology, typical of dedifferentiated chondrocytes, and cells in HA-PEGDA showing a spherical shape, typical of native chondrocytes, as shown by calcein staining (Fig. S3). Additionally, we verified the expression of chondrocyte-specific markers after 4 and 10 days of culture in the different hydrogels (Fig. 3E and F). In fibrin, chondrocytes resulted negative for Collagen-II and Aggrecan even after 10 days. On the contrary, both these markers were expressed in all the HA-based hydrogels in different amounts. Chondrocytes cultured in HA-PEGDA showed the strongest expression already at day 4, which further increased at day 10.

3.3. Mimicking an OA environment in the joint-on-a-chip

To generate an OA-like microenvironment, synovial fibroblasts and chondrocytes were cultured in fibrin and HA-PEGDA respectively. The effect of OA-SynFlu was assessed in comparison with culture medium (named "Medium" in the figures).

The presence of OA-SynFlu significantly increased the viability of both synovial fibroblasts and articular chondrocytes at day 4 ($p < 0.01$) compared to medium (Fig. 4A). At day 10, the viability of synovial fibroblasts cultured in OA-SynFlu dropped below 75 %, being slightly lower than that observed in the presence of medium. A slight decrease in cell viability over time was observed also in articular chondrocytes cultured in OA-SynFlu, which however displayed significantly higher viability compared to the chondrocytes cultured in medium ($p < 0.01$) at day 10. On the other hand, OA-SynFlu induced cell senescence both in synovial fibroblasts and in articular chondrocytes, as shown by the significantly higher fraction of SA-β-Galactosidase positive cells observed at 10 days in the presence of OA-SynFlu than in culture medium (Fig. 4B). We also evaluated the expression of matrix-related synovial fibroblast and chondrocyte markers after 10 days of culture. In synovial fibroblasts, Collagen-I was expressed at similar levels in the presence of medium and OA-SynFlu, (Fig. 4C), whilst Lubricin was slightly reduced by OA-SynFlu. In articular chondrocytes, Collagen-II expression was slightly higher in the presence of OA-SynFlu, than in culture medium (Fig. 4C). Differently, Aggrecan and Collagen-I expression was similar in chips cultured with culture medium and OA-SynFlu (Fig. 4C).

To confirm the generation of a pro-inflammatory environment within the joint-on-a-chip model cultured with OA-SynFlu, we quantified the concentration of pro- and anti-inflammatory cytokines. In our devices, cytokine concentration resulted higher in OA-SynFlu models as compared to chips cultured with medium, with IL1α, IL6, IL8, and TNFα presenting the highest concentrations (Fig. 5A). Remarkably, these cytokines were more abundant in the devices than in the original OA-SynFlu, suggesting that cells actively secreted pro-inflammatory cytokines in the presence of OA-SynFlu. To further evaluate the specific contribution of synovial fibroblasts and chondrocytes in cytokine production, we quantified IL8 and TNFα present within cell cytoplasm through immunofluorescence staining of the respective chip compartments (Fig. 5B). IL8 was absent in both cell types in the presence of culture medium and was significantly induced by OA-SynFlu both in chondrocytes and in synovial fibroblasts. Differently, TNFα was produced by both cell types even in the presence of only culture medium, and the addition of OA-SynFlu significantly increased its production only in synovial fibroblasts (Fig. 5C). Finally, we assessed the expression of matrix metalloproteinases (MMP1 and MMP13) as relevant markers of the matrix degradative process. In both synovial fibroblasts and articular chondrocytes, the expression of MMP1 and MMP13 was significantly higher in devices cultured with OA-SynFlu compared to culture medium (Fig. 6).

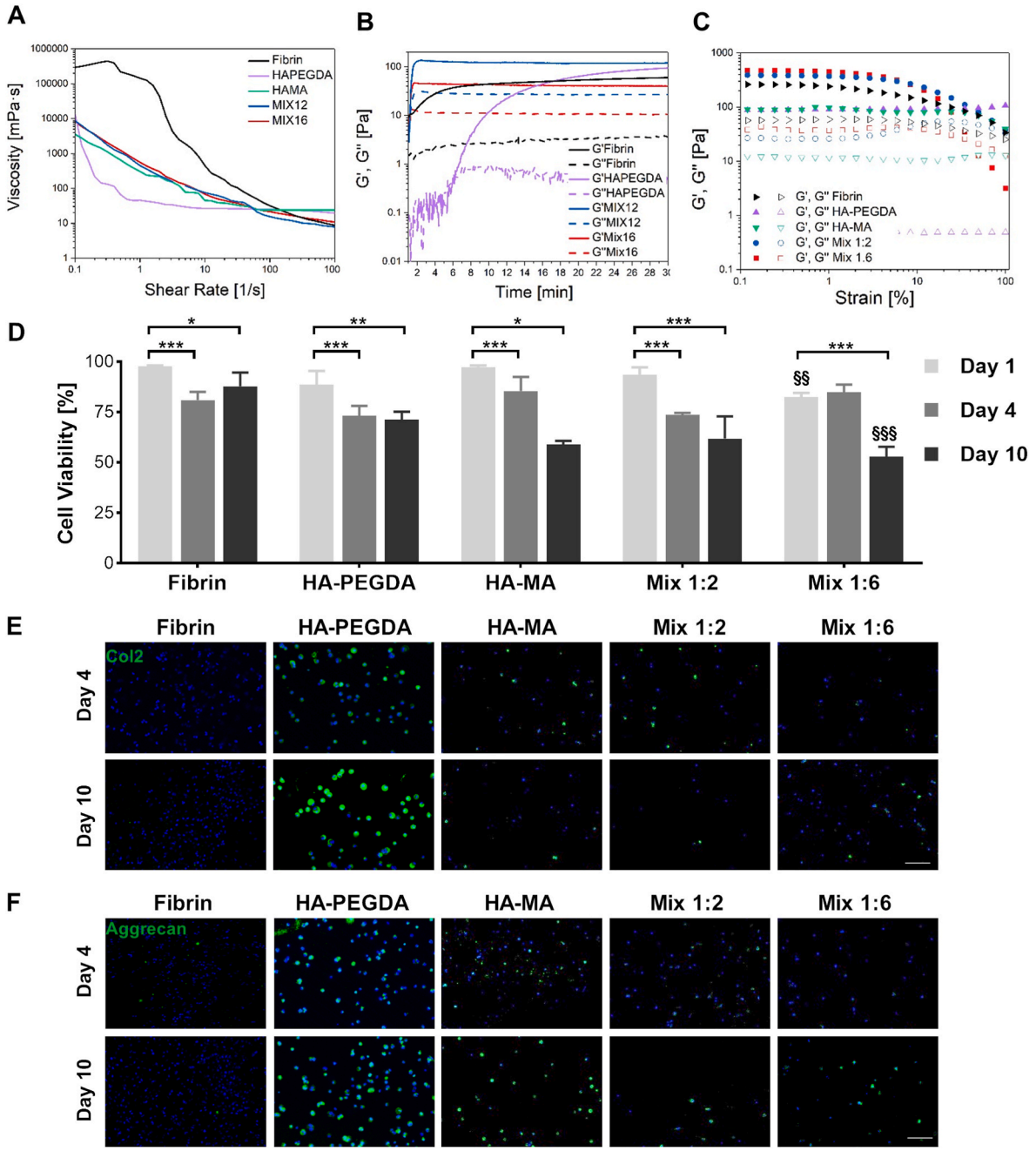

Fig. 3. Comparison of different hydrogels for the cartilage compartment. **(A)** Graph showing the hydrogel viscosity as a function of applied shear rate, **(B)** time sweep curves measured during hydrogel polymerization, and **(C)** G′ and G″ moduli of the tested hydrogels. **(D)** Chondrocyte viability in the hydrogels after 1, 4, and 7 days of culture (n = 3; *p < 0.05, **p < 0.01, ***p < 0.001 as compared to the same gel at day 1; §§p < 0.01, §§§: p < 0.001 as compared to fibrin at the same day). **(E,F)** Expression of Collagen-II (Col2) and Aggrecan (both in green) at day 4 and 10. Nuclei are stained with DAPI (blue). Scale bars: 100 μm. (For interpretation of the references to colour in this figure legend, the reader is referred to the Web version of this article.)

Altogether, these results demonstrate that OA-SynFlu generated a catabolic OA microenvironment in the system, inducing typical OA hallmarks such as the secretion of proinflammatory cytokines and increased production of degradative enzymes by articular cells.

3.4. Patient-specific OA joint-on-a-chip models

Lastly, we evaluated the possibility to exploit our OA joint-on-a-chip model as a potential screening tool for a personalized monitoring of orthobiologics efficacy. In these experiments, personalized models were generated using donor-matched synovial fibroblasts, articular chondrocytes, and synovial fluid obtained from 3 OA patients. An allogeneic injective therapy was simulated adding the same BMSCs and ASCs in the synovial fluid channel.

To measure cytokine baseline values, we first quantified the cytokine concentration in the original OA-SynFlu samples collected from patients. The values displayed a similar pattern of cytokine content among the donors (Fig. 7A). In line with the cytokine quantification in OA-SynFlu pooled from multiple patients, IL-6, IL-8, and TNF-α were the most expressed in all patients, with the OA-SynFlu from Patient 3 showing the highest concentrations of these markers.

The quantification of cytokines in the SynFlu collected from the devices after cell injection showed that patient-specific models responded differently to the treatment with MSCs (Fig. 7B). Overall, Patient 1

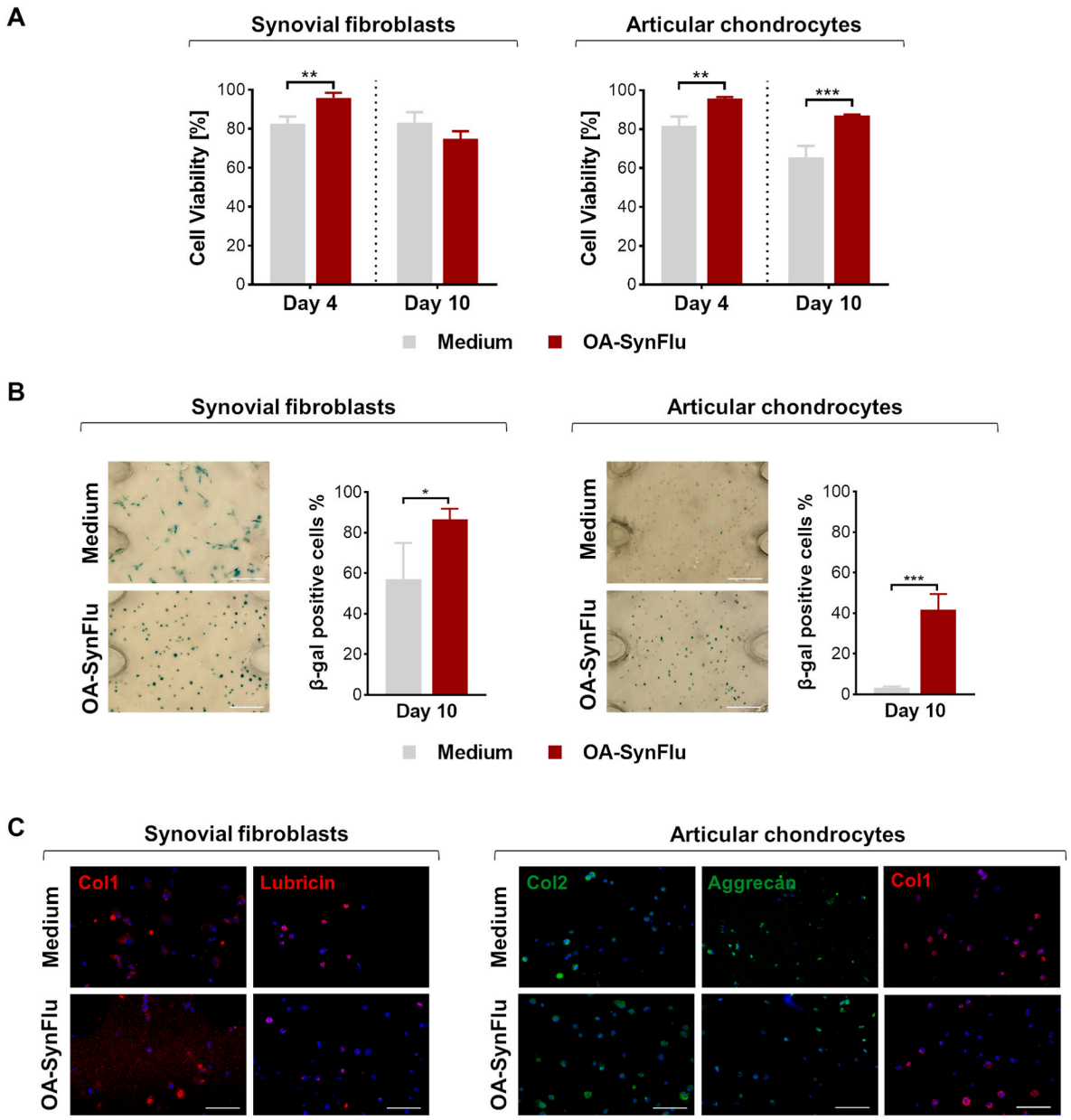

Fig. 4. Evaluating the effects of OA-SynFlu on cells within the joint-on-a-chip model. **(A)** Viability of synovial fibroblasts and chondrocytes after 4 and 10 days of culture in the presence of Culture Medium or OA-SynFlu. Cell viability is expressed as the percentage of live cells over the total number of cells ($n = 3$; $^{**}p < 0.01$). **(B)** Assessment of synovial fibroblasts and chondrocyte senescence through SA-β-Galactosidase activity assay. The result is expressed in terms of percentage of positive cells over total cells ($n = 4$; $^{*}p < 0.05$; $^{***}p < 0.001$). **(C,D)** Expression of tissue-specific markers in synovial fibroblasts (Col1 and Lubricin in red, nuclei in blue) and articular chondrocytes (Col2 and Aggrecan in green and Col1 in red, nuclei in blue) cultured in the presence of Culture Medium or OA-SynFlu in the chip. Scale bars: 100 μm. (For interpretation of the references to colour in this figure legend, the reader is referred to the Web version of this article.)

seemed the most responsive to both BMSCs and ASCs injection, presenting a decrease of IL6, IL8, IL4 and IL10 and an increase of IL13 and TNFα in both cases. IL1α and IFNγ were modulated only by BMSCs, evidencing a slight difference between the two treatments. In Patient 2 the injection of either cells induced a decrease in IFNγ and TNFα and an increase in IL6. BMSCs and ASCS seemed however to elicit different anti-inflammatory responses, since BMSCs increased the secretion of anti-inflammatory cytokines IL4 and IL10, whilst ASCs downregulated inflammatory cytokines IL1α and IL1β. Lastly, Patient 3 had no response to cell injection, since most cytokine concentrations resulted similar to the control condition, with the exception of IL1α and IL1β.

The quantification of MMP1 and MMP13 signals in patient-specific models from 3 OA patients is shown in Fig. 7C. In Patient 1, both BMSCs and ASCs significantly decreased the expression of MMP1 ($p < 0.001$) and MMP13 ($p < 0.001$) in articular chondrocytes and synovial fibroblasts. The decreased production of degradative enzymes, associated with a higher modulation of cytokine production, both suggested a responsivity of Patient 1 to the treatment with BMSCs and ASCs (Fig. 7D). In general, Patient 2 and 3 showed lower starting levels of both MMP1 and MMP13 compared to Patient 1. This might explain why the treatment with both BMSCs and ASCs did not yield relevant effects in terms of MMP down-regulation. Indeed, a small decrease in MMP1 levels was found only in Patient 2 samples treated with ASCs ($p < 0.05$). Unexpectedly, the levels of MMP1 were increased upon BMSC treatment in Patient 3 ($p < 0.001$).

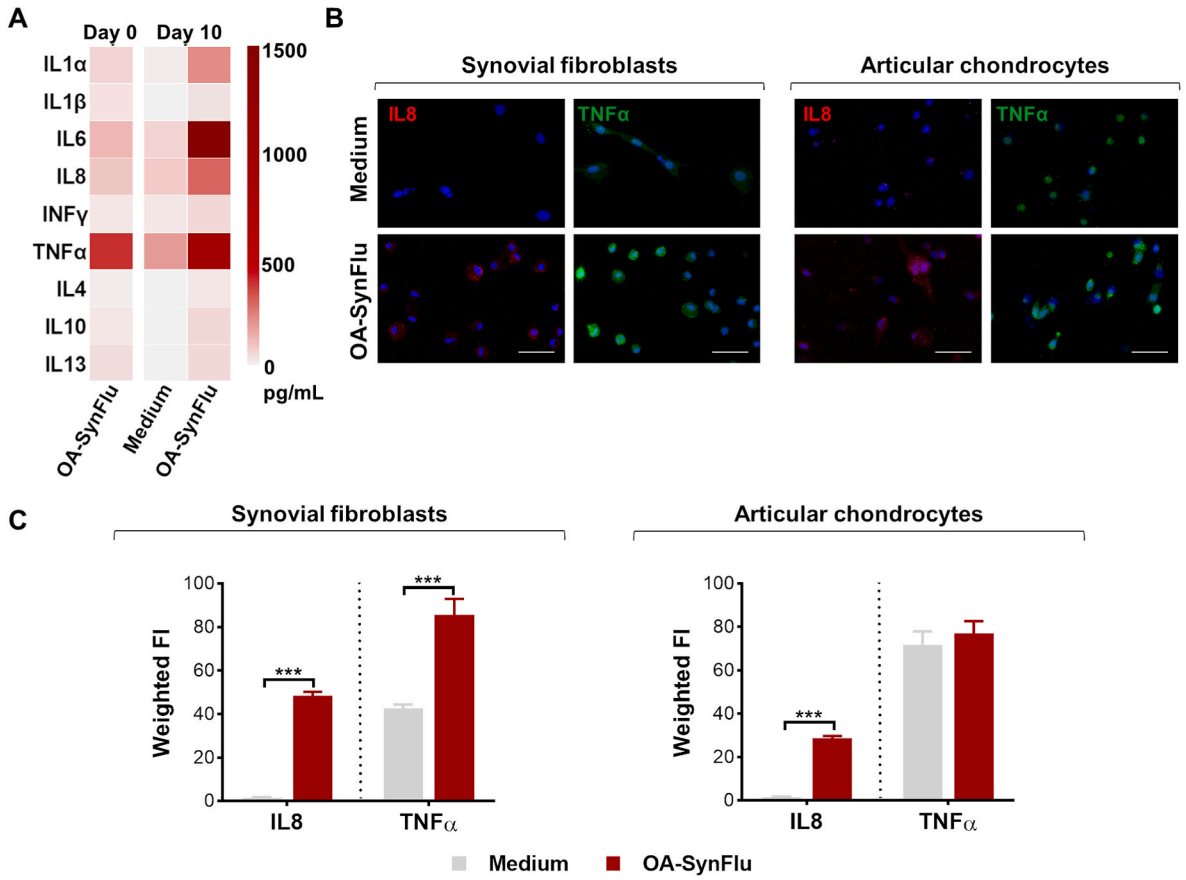

Fig. 5. Verifying the induction of a pro-inflammatory microenvironment with OA-SynFlu in the joint-on-a-chip model.**(A)** Heatmap showing cytokine content in pooled OA-SynFlu at day 0 and in the supernatants collected at day 10 and pooled from 3 independent chips cultured with Culture Medium or OA-SynFlu. **(B)** Representative immunofluorescence images of IL8 (red) and TNFα (green) in synovial fibroblasts and articular chondrocytes. Nuclei are stained with DAPI (blue). Scale bars: 100 μm. **(C)** Quantification of IL8 and TNFα signal in the presence of Culture Medium and OA-SynFlu (n = 3; ***p < 0.001). (For interpretation of the references to colour in this figure legend, the reader is referred to the Web version of this article.)

4. Discussion

Although synovial inflammation plays a crucial role in the onset and progression of OA pathology [16], only a few microfluidic joint models have included a synovial membrane compartment so far [17]. In our study, we embedded synovial fibroblasts from OA patients in fibrin to replicate the pathological synovium environment. Our results demonstrate that synovial fibroblasts were highly viable and maintained their phenotype [17] when cultured in a fibrin matrix, expressing Collagen-I, as already reported for synovial membrane fibroblasts [18]. Lubricin (also known as PRG4), a specific marker of synovial fibroblasts representing a major component of the synovial fluid crucial for joint lubrication [19], was also expressed by synovial fibroblasts embedded in fibrin, indicating that this hydrogel, widely applied in microfluidic models due to its high biocompatibility, versatility and ease-of-handling, is suitable for the 3D culture of synovial fibroblasts. Differently, preliminary experiments conducted culturing articular chondrocytes in fibrin revealed that a short-term culture in fibrin in the absence of any chondrogenic factor was not able to support the expression of cartilage-specific markers, prompting us to test different hydrogels for the cartilage compartment. For a faithful reproduction of a cartilage-like environment, a crucial role is indeed played by the extracellular matrix (ECM), that in cartilage is composed by a blend of Collagen and HA [20]. Although HA-based hydrogels have been widely applied as cartilage/osteochondral tissue engineering scaffolds, showing the ability to support chondrogenic differentiation and leading to cartilaginous tissue both *in vitro* [21] and in vivo [22], they have not been exploited yet in joint-on-a-chip models [20]. In our work, we selected gels mimicking cartilage ECM composition, firstly verifying their compatibility with chip injection. Gelation times of all the tested gels was sufficiently long to allow injection before complete polymerization, in accordance with the literature [23]. We then tested the mechanical properties of different gel compositions, showing that G′ was lower than 500 Pa for all the tested hydrogels. The highest G′ value of MIX hydrogels was not surprising, considering the dual nature of their crosslinking (i.e. physical (temperature) and chemical (UV)). For these gels, the significantly lower values of G′ after physical crosslinking as compared to G′ values after UV exposure indicated a predominant effect of the photocrosslinking on the viscoelastic properties. Furthermore, collagen content of MIX gels influenced the mechanical properties of the gels, since MIX 1:2 showed higher storage modulus (G′) values than MIX 1:6, compatibly with the higher collagen content of the former [24]. Although all G′ values are far from the compressive modulus of articular cartilage (0.02–1.16 MPa in the superficial zone and 6.44–7.75 MPa in the deep zone [25]), most of the hydrogels developed for cartilage engineering have similar compression moduli [20]. In this context, several works have investigated the effect of matrix stiffness on chondrocyte behavior, reporting conflicting outcomes [26]. In particular, it has been demonstrated that MSC embedded in a HA-PEGDA hydrogel with a storage modulus ranging from 135 to 185 Pa promoted a complete repair of a full-thickness cartilage lesion in rats and that an increase in the material stiffness resulted in poor chondrogenesis, driving MSC differentiation towards bone cells [27]. We observed a decrease in chondrocyte viability over time in our hydrogels, although at day 10 the number of viable chondrocytes was still above 70 % for HA-PEGDA, close to literature data [28], and confirming HA-PEGDA

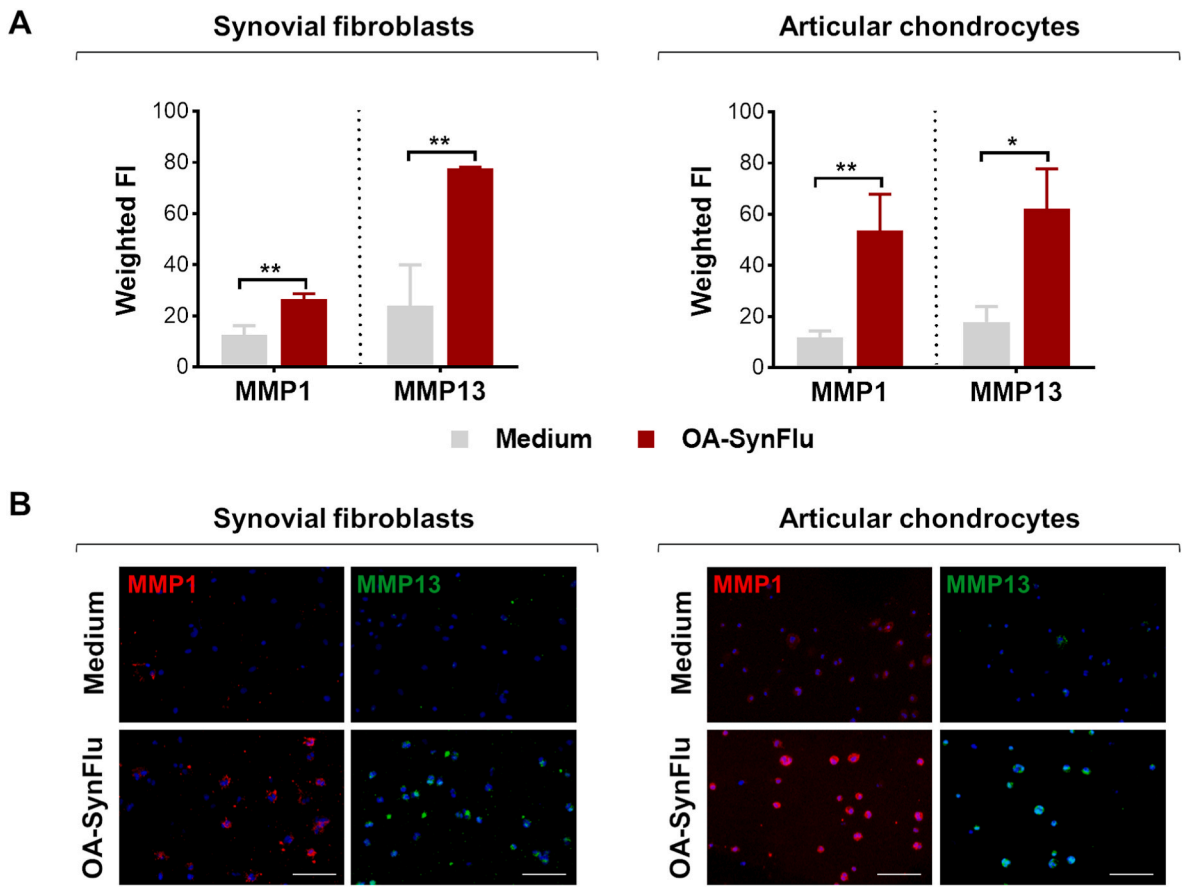

Fig. 6. Assessment of the pro-degradative microenvironment in presence of OA-SynFlu in the microfluidic model. **(A)** Quantification of MMP1 and MMP13 signal (n = 3; *p < 0.05, **p < 0.01). **(B)** Expression of matrix metalloproteinases (MMP1 in red and MMP13 in green) in the presence of Culture Medium or OA-SynFlu in synovial fibroblasts and articular chondrocytes. Scale bars: 100 μm. (For interpretation of the references to colour in this figure legend, the reader is referred to the Web version of this article.)

cytocompatibility. Methacrylated hydrogels (HA-MA and MIX formulations), showed a more marked decrease in cell viability, possibly related to the presence of residual crosslinker, as speculated in previous studies reporting a reduction of chondrocyte viability to 60 % in HA-MA [29] and to 50 % HA-MA/GelMa gels [30]. Although UV-based polymerization is faster compared to enzymatic or chemical polymerization, the potential residual cytotoxicity of the chemical crosslinker, especially in microfluidic devices with limited mass transport [31], can lead to low cell viability, in line with our findings. This aspect can possibly limit the application of UV-photocrosslinkable hydrogels in microfluidic systems. Besides showing higher viability, HA-PEGDA embedded chondrocytes also expressed higher levels of Collagen-II and Aggrecan. This improved chondrocyte differentiation was not due to differences in matrix stiffness as reported in other works [32], since similar G' values were measured for all the tested hydrogel. Although improved chondrogenic differentiation has been reported also for HA-MA gels [21] and hydrogels combining GelMA and HA-MA [30,33], in our study these gels induced weaker expression of chondrogenic markers compared to HA-PEGDA. The short culture timeframe and the lack of chondrogenic factors in the medium can, at least partially, account for the poor performance of HA-MA-based hydrogels in our experimental set-up, compared to literature data.

A limitation of our model is the absence of macrophages in the synovial compartment, which was due to the impossibility to isolate a sufficient number of macrophages from the synovial membrane biopsies or from a peripheral blood sample obtained from the same patients. However, the use of synovial fluid from OA patients in the model still allowed to monitor the effects on fibroblasts and chondrocytes of pro-inflammatory mediators, which in vivo are released in the synovial fluid both from articular cells and from macrophages resident and/or infiltrated in the synovial membrane. Our approach in fact differs from other OA joint-on-a-chip models, which rely on mechanical overload [11] or chemicals [34] to drive OA onset, with the disadvantage of considering a single factor as disease-inducing stimulus.

The addition of OA-SynFlu modified the behavior of joint cells in our system, causing a hyperproliferation of chondrocytes, an early event occurring in OA onset [35], and showing a cytotoxic effect in fibroblasts. Studies on synovial fibroblasts in OA conditions reported an inflammation-induced cell death [36], in accordance with our findings. Besides the effects on cell viability, we observed an increase in cytokine production, in line with the reported increase of IL6, IL8 and TNFα in 2D cultures of chondrocytes exposed to OA-SynFlu [37] and in SynFlu and plasma of arthritic patients [38]. Interestingly, some of these cytokines were increased by OA-SynFlu in both cell types, whilst others such as TNFα, were upregulated only in synovial fibroblasts, highlighting a different effect of OA-SynFlu on articular cells. Furthermore, we observed an increase in cell senescence in both cell types in response to OA-SynFlu, which can be associated to the augmented levels of IL8, MMP1 and MMP13, major components of the senescence-associated secretory phenotype. We highlighted also a modification of differentiation markers and catabolic enzymes production with the addition of OA-SynFlu in our chip. An increase of Collagen-I transcriptional expression has been highlighted during OA onset [39], supporting the activation of a de-differentiation process in OA chondrocytes. On the contrary, we did not evidence an increase in Collagen-I in synovial fibroblasts, in contrast with other literature reports. The difference is

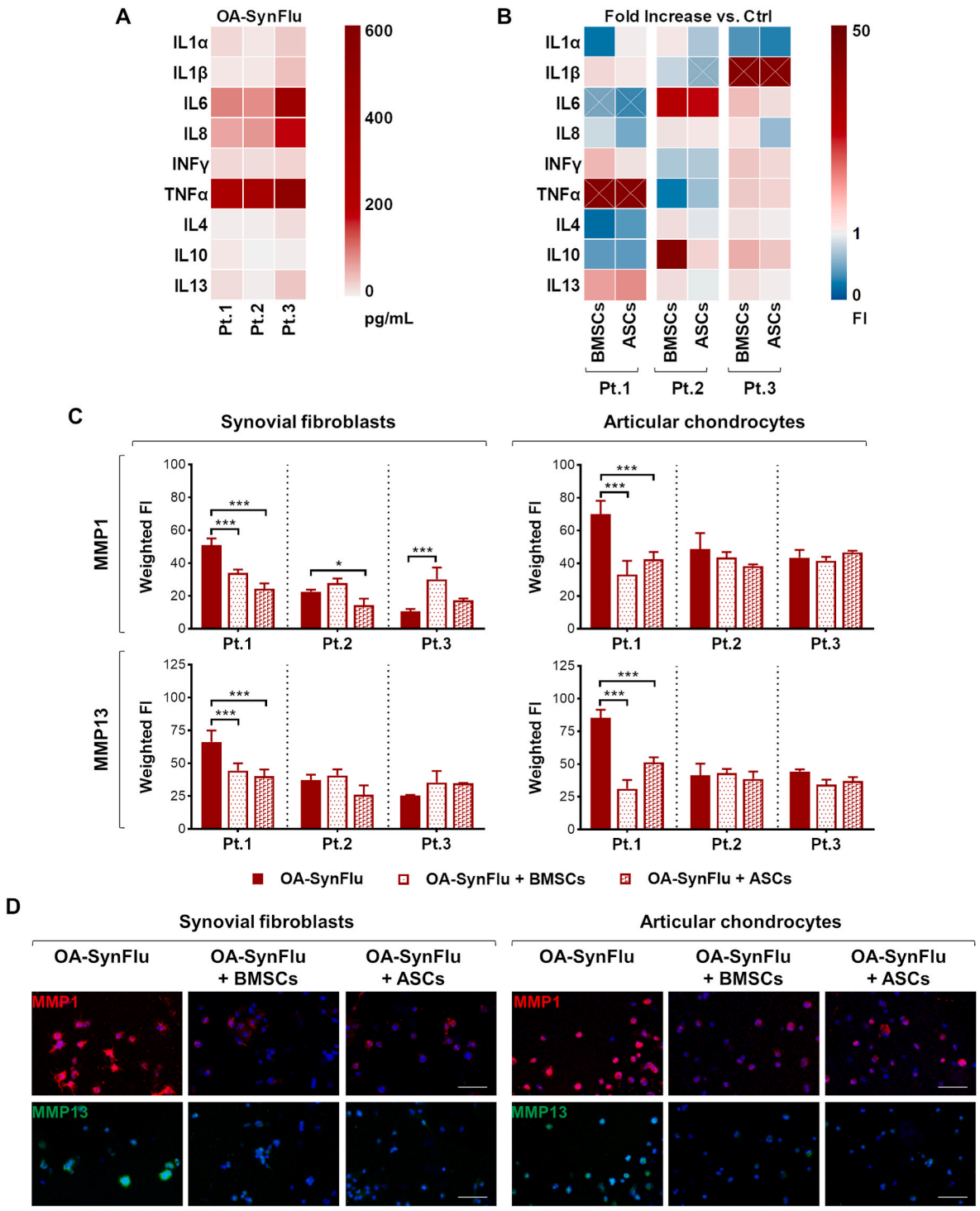

Fig. 7. Patient-specific OA joint-on-a-chip models as screening platforms for biological treatments. **(A)** Cytokine quantification in OA-SynFlu from Patients 1–3. **(B)** Fold increase for each cytokine measured in patient-specific models in the presence of BMSCs (OA-SynFlu + BMSCs) and ASCs (OA-SynFlu + ASCs) normalized with respect to the control condition (OA-SynFlu) set at 1. For each condition, supernatants were pooled from 3 independent chips. White crosses in the heatmap indicate that one of the values used to calculate the fold increase fell below the sensitivity range of the assay. In this case, to estimate the fold increase, we used a value that was half of the lower standard curve limit. **(C)** Quantification of MMP1 and MMP13 in patient-specific joint-on-a-chip models, non-treated or treated with BMSCs or ASCs ($n = 3$; *$p < 0.05$, **$p < 0.01$, ***$p < 0.001$). **(D)** Representative images of MMP1 (red) and MMP13 (green) for Patient 1. Nuclei are stained with DAPI (blue). Scale bars: 100 μm. (For interpretation of the references to colour in this figure legend, the reader is referred to the Web version of this article.)

possibly due to the short timeframe in our model compared to the insurgence of synovial fibrosis, which takes place in end-stage phases of the disease [40]. The duration of our experiments was in fact limited to 10 days due to the high remodeling of the fibrin matrix from synovial fibroblasts, leading to gel degradation and subsequent cell migration into the central channel at longer time points.

MMP1 and MMP13 are two of the major effectors of cartilage degradation, being able to cleave the C-terminus of Aggrecan and degrade Collagen-II [41]. We showed an increase of both enzymes in synovial fibroblasts and chondrocytes in response to OA synovial fluid,

in line with other literature studies reporting the upregulation of matrix metalloproteinases in chondrocytes and in co-cultures of synovial fibroblasts and chondrocytes primed with OA synovial fluid or inflammatory mediators [42,43]. Finally, in a proof-of-concept experiment, we tested the possibility to exploit our OA joint-on-a-chip as a personalized assay for the screening of anti-OA therapies, evaluating the effects of the injection of mesenchymal cells (MSCs). This promising approach mainly relies on the secretion of a huge amount of immunomodulatory and trophic factors by MSCs, acting as a sort of "drugstore" [44], rather than on their multi-differentiative capacities. Although MSCs have already been used in several clinical approaches [45], how their efficacy may depend on patient-specific factors remains to be clarified. Previous works highlighted a high inter-donor variability in terms of cytokine content of OA-SynFlu [46] or features of articular chondrocytes [14]. BMSC features have also been shown to change according to the arthritic stage of the synovial fluid they are exposed to [47] and similarly, the anti-inflammatory capabilities of these cells are known to vary based on the inflammation grade of the surrounding articular cells [48]. In this context, conflicting results have been reported on the effects of MSCs on OA chondrocytes and/or synovial fibroblasts, since either a decreased expression of MMP1 and MMP13 after BMSC treatment [49] or no effects with MSC addition [50] have been reported. Furthermore, chondrocytes co-cultured with BMSCs and ASCs *in vitro* showed a lower expression of pro-inflammatory cytokines, such as IL1β, IL6, IL8, and TNFα [48] but also an increase of MSCs production of IL6 in the presence of OA-SynFlu has been reported [47]. The short treatment timeframe of our experiments allowed us to evaluate only fast-occurring modifications of the system such as the reduction of inflammatory cytokines and the alterations in the production of MMP1 and MMP13 that are reported to occur in a few days [51], but not later events such as ECM regeneration. Both MMP1 and MMP13 are involved in the breakdown of Collagen, with MMP13 specifically targeting Collagen II. MMP-13, predominantly expressed by chondrocytes, is upregulated in OA and is associated with the proteolytic processes leading to cartilage degradation in OA [52]. Similarly, elevated levels of MMP1 are often observed in OA, and are recognized to contribute to cartilage degradation. MMP-1 is produced by various cells, including synovial fibroblasts and articular chondrocytes [53], and its activation is considered a key event in the pathological process leading to cartilage breakdown [54]. Altogether, our findings show how each patient-specific model displays a different behavior in terms of cytokine modulation and degradative enzyme production, depending on the patient-specific combination of articular cells and synovial fluid, since the same MSCs were injected in all patients. A high inter-donor variability emerged from our data, highlighting how personalized models can be more predictive of the treatment outcome. Nevertheless, we do not envisage an approach in which patient-specific models can be used for the benefit of the single patient, rather, they can be used for the stratification of OA patients, and this could be useful for better targeting the clinical application of MSCs, albeit our results are limited to a very small number of donors. To overcome this hurdle, a higher number of donors will be needed to validate the chip as a screening platform. It should be highlighted that a major limitation of this study resides in the inclusion of only two tissue compartments in the system. Subchondral bone is indeed known to strictly interact with the cartilage compartment and is subjected to important changes during OA. However, the complexity of organotypic models should be finely balanced to avoid overcomplicating the system, which may pose significant challenges in terms of model reproducibility and reliability [55]. Hence, here we decided to focus on synovium and cartilage compartments which in the joint are in direct contact with synovial fluid and are directly targeted by the action of MSCs when injective treatments are applied to the joint. However, despite falling beyond the scope of this specific study, the inclusion of bone in the system might represent a significant advancement to increase the relevance of this model.

In conclusion, we developed a joint-on-chip model based on a hydrogel mimicking the composition of the cartilage extracellular matrix to promote the maintenance of chondrocyte viability and phenotype. Adding synovial fluid from OA patients allowed reproducing some hallmarks of OA disease, such as increased cell senescence, production of inflammatory cytokines and matrix degradation enzymes. The proof-of-concept application of a patient-specific model allowed screening the effects of MSCs injection on OA signatures, evidencing a high dependence of treatment efficacy on patient characteristics.

Funding

This project was funded by the Advisory Board of Research of Ente Ospedaliero Cantonale (ABREOC) and by the Italian Ministry of Health (Ricerca Corrente).

CRediT authorship contribution statement

Dalila Petta: Writing – original draft, Methodology, Investigation, Conceptualization. **Daniele D'Arrigo:** Writing – original draft, Methodology, Investigation, Conceptualization. **Shima Salehi:** Investigation, Methodology, Visualization, Writing - review & editing **Giuseppe Talò:** Visualization, Methodology. **Lorenzo Bonetti:** Writing – original draft, Methodology. **Marco Vanoni:** Supervision. **Luca Deabate:** Resources. **Luigi De Nardo:** Supervision. **Gabriele Dubini:** Supervision. **Christian Candrian:** Funding acquisition. **Matteo Moretti:** Supervision, Funding acquisition, Conceptualization. **Silvia Lopa:** Writing – review & editing, Visualization, Data curation, Conceptualization. **Chiara Arrigoni:** Writing – review & editing, Project administration, Data curation, Conceptualization.

Declaration of competing interest

The authors declare that they have no known competing financial interests or personal relationships that could have appeared to influence the work reported in this paper.

Data availability

The datasets generated during the current study are available in OSF at the following link (DOI 10.17605/OSF.IO/WQNHR):https://osf.io/wqnhr/?view_only%20=%20f5afd0bd862b45b88c97d0a774303ded.

Appendix A. Supplementary data

Supplementary data to this article can be found online at https://doi.org/10.1016/j.mtbio.2024.101072.

References

[1] D.J. Hunter, S. Bierma-Zeinstra, Osteoarthritis, Lancet 393 (2019) 1745–1759, https://doi.org/10.1016/S0140-6736(19)30417-9.
[2] A.R. Poole, Osteoarthritis as a whole joint disease, HSS J. 8 (2012) 4–6, https://doi.org/10.1007/S11420-011-9248-6.
[3] J. Sellam, F. Berenbaum, The role of synovitis in pathophysiology and clinical symptoms of osteoarthritis, Nat. Rev. Rheumatol. 6 (2010) 625–635, https://doi.org/10.1038/nrrheum.2010.159.
[4] A.E. Weber, I.K. Bolia, N.A. Trasolini, Biological strategies for osteoarthritis: from early diagnosis to treatment, Int. Orthop. 45 (2021) 335–344, https://doi.org/10.1007/S00264-020-04838-W.
[5] S. Lopa, A. Colombini, M. Moretti, L. de Girolamo, Injective mesenchymal stem cell-based treatments for knee osteoarthritis: from mechanisms of action to current clinical evidences, Knee Surg. Sports Traumatol. Arthrosc. 27 (2019) 2003–2020, https://doi.org/10.1007/S00167-018-5118-9.
[6] M. Leist, T. Hartung, Inflammatory findings on species extrapolations: humans are definitely no 70-kg mice, Arch. Toxicol. 87 (2013) 563–567, https://doi.org/10.1007/S00204-013-1038-0.
[7] M. Rothbauer, E.I. Reihs, A. Fischer, R. Windhager, F. Jenner, S. Toegel, A progress report and roadmap for microphysiological systems and organ-on-A-chip technologies to Be more predictive models in human (knee) osteoarthritis, Front. Bioeng. Biotechnol. 10 (2022), https://doi.org/10.3389/FBIOE.2022.886360.

[8] S. Bersini, C. Arrigoni, S. Lopa, M. Bongio, I. Martin, M. Moretti, Engineered miniaturized models of musculoskeletal diseases, Drug Discov. Today (2016), https://doi.org/10.1016/j.drudis.2016.04.015.

[9] S. Piluso, Y. Li, F. Abinzano, R. Levato, L. Moreira Teixeira, M. Karperien, J. Leijten, R. van Weeren, J. Malda, Mimicking the articular joint with in vitro models, Trends Biotechnol. 37 (2019) 1063–1077, https://doi.org/10.1016/J.TIBTECH.2019.03.003.

[10] C. Mondadori, S. Palombella, S. Salehi, G. Talo, R. Visone, M. Rasponi, A. Redaelli, V. Sansone, M. Moretti, S. Lopa, Recapitulating monocyte extravasation to the synovium in an organotypic microfluidic model of the articular joint, Biofabrication 13 (2021), https://doi.org/10.1088/1758-5090/AC0C5E.

[11] P. Occhetta, A. Mainardi, E. Votta, Q. Vallmajo-Martin, M. Ehrbar, I. Martin, A. Barbero, M. Rasponi, Hyperphysiological compression of articular cartilage induces an osteoarthritic phenotype in a cartilage-on-a-chip model, Nat. Biomed. Eng. 3 (2019) 545–557, https://doi.org/10.1038/S41551-019-0406-3.

[12] V. Graceffa, C. Vinatier, J. Guicheux, M. Stoddart, M. Alini, D.I. Zeugolis, Chasing Chimeras-The elusive stable chondrogenic phenotype. https://doi.org/10.1016/j.biomaterials.2018.11.014, 2018.

[13] S. Treppo, H. Koepp, E.C. Quan, A.A. Cole, K.E. Kuettner, A.J. Grodzinsky, Comparison of biomechanical and biochemical properties of cartilage from human knee and ankle pairs, J. Orthop. Res. 18 (2000) 739–748, https://doi.org/10.1002/jor.1100180510.

[14] M. Lagana, C. Arrigoni, S. Lopa, V. Sansone, L. Zagra, M. Moretti, M.T. Raimondi, M. Laganà, C. Arrigoni, S. Lopa, V. Sansone, L. Zagra, M. Moretti, M.T. Raimondi, Characterization of articular chondrocytes isolated from 211 osteoarthritic patients, Cell Tissue Bank. (2014), https://doi.org/10.1007/s10561-013-9371-3.

[15] M.C. Tanzi, S. Farè, Characterization of polymeric biomaterials. https://doi.org/10.1016/C2015-0-01988-8, 2017.

[16] A. Mathiessen, P.G. Conaghan, Synovitis in osteoarthritis: current understanding with therapeutic implications, Arthritis Res. Ther. 19 (2017), https://doi.org/10.1186/S13075-017-1229-9.

[17] H.S. Choi, C.J. Ryu, H.M. Choi, J.S. Park, J.H. Lee, K. Il Kim, H.I. Yang, M.C. Yoo, K.S. Kim, Effects of the pro-inflammatory milieu on the dedifferentiation of cultured fibroblast-like synoviocytes, Mol. Med. Rep. 5 (2012) 1023–1026, https://doi.org/10.3892/MMR.2012.767.

[18] F. Li, Y. Tang, B. Song, M. Yu, Q. Li, C. Zhang, J. Hou, R. Yang, Nomenclature clarification: synovial fibroblasts and synovial mesenchymal stem cells, Stem Cell Res. Ther. 10 (2019), https://doi.org/10.1186/S13287-019-1359-X.

[19] G.D. Jay, D.E. Britt, C.J. Cha, Lubricin is a product of megakaryocyte stimulating factor gene expression by human synovial fibroblasts, J. Rheumatol. 27 (2000) 594–600.

[20] D. Petta, U. D'Amora, D. D'Arrigo, M. Tomasini, C. Candrian, L. Ambrosio, M. Moretti, Musculoskeletal tissues-on-a-chip: role of natural polymers in reproducing tissue-specific microenvironments, Biofabrication 14 (2022), https://doi.org/10.1088/1758-5090/AC8767.

[21] V.H.M. Mouser, A. Abbadessa, R. Levato, W.E. Hennink, T. Vermonden, D. Gawlitta, J. Malda, Development of a thermosensitive HAMA-containing bio-ink for the fabrication of composite cartilage repair constructs, Biofabrication 9 (2017), https://doi.org/10.1088/1758-5090/AA6265.

[22] J. Chen, J. Yang, L. Wang, X. Zhang, B.C. Heng, D.A. Wang, Z. Ge, Modified hyaluronic acid hydrogels with chemical groups that facilitate adhesion to host tissues enhance cartilage regeneration, Bioact. Mater. 6 (2020) 1689–1698, https://doi.org/10.1016/J.BIOACTMAT.2020.11.020.

[23] X.Z. Shu, Y. Liu, F.S. Palumbo, Y. Luo, G.D. Prestwich, In situ crosslinkable hyaluronan hydrogels for tissue engineering, Biomaterials 25 (2004) 1339–1348, https://doi.org/10.1016/j.biomaterials.2003.08.014.

[24] M. Shayegan, N.R. Forde, Microrheological characterization of collagen systems: from molecular solutions to fibrillar gels, PLoS One 8 (2013), https://doi.org/10.1371/JOURNAL.PONE.0070590.

[25] S.S. Chen, Y.H. Falcovitz, R. Schneiderman, A. Maroudas, R.L. Sah, Depth-dependent compressive properties of normal aged human femoral head articular cartilage: relationship to fixed charge density, Osteoarthritis Cartilage 9 (2001) 561–569, https://doi.org/10.1053/JOCA.2001.0424.

[26] E. Schuh, S. Hofmann, K.S. Stok, H. Notbohm, R. Müller, N. Rotter, The influence of matrix elasticity on chondrocyte behavior in 3D, J Tissue Eng Regen Med 6 (2012), https://doi.org/10.1002/term.501.

[27] J. Li, Y. Huang, J. Song, X. Li, X. Zhang, Z. Zhou, D. Chen, P.X. Ma, W. Peng, W. Wang, G. Zhou, Cartilage regeneration using arthroscopic flushing fluid-derived mesenchymal stem cells encapsulated in a one-step rapid cross-linked hydrogel, Acta Biomater. 79 (2018) 202–215, https://doi.org/10.1016/J.ACTBIO.2018.08.029.

[28] A.K. Scott, E. Casas, S.E. Schneider, A.R. Swearingen, C.L. Van Den Elzen, B. Seelbinder, J.E. Barthold, J.F. Kugel, J.L. Stern, K.J. Foster, N.C. Emery, J. Brumbaugh, C.P. Neu, C.L. Van Den Elzen, B. Seelbinder, J.E. Barthold, J. F. Kugel, J.L. Stern, K.J. Foster, N.C. Emery, J. Brumbaugh, C.P. Neu, Epigenetic remodeling during monolayer cell expansion reduces therapeutic potential. https://doi.org/10.1101/2021.12.14.472696, 2021.

[29] J.W.S. Hayami, S.D. Waldman, B.G. Amsden, Chondrocyte generation of cartilage-like tissue following photoencapsulation in methacrylated polysaccharide solution blends, Macromol. Biosci. 16 (2016) 1083–1095, https://doi.org/10.1002/MABI.201500465.

[30] S. Pahoff, C. Meinert, O. Bas, L. Nguyen, T.J. Klein, D.W. Hutmacher, Effect of gelatin source and photoinitiator type on chondrocyte redifferentiation in gelatin methacryloyl-based tissue-engineered cartilage constructs, J. Mater. Chem. B 7 (2019) 1761–1772, https://doi.org/10.1039/C8TB02607F.

[31] A.E. Kamholz, B.H. Weigl, B.A. Finlayson, P. Yager, Quantitative analysis of molecular interaction in a microfluidic channel: the T-sensor, Anal. Chem. 71 (1999) 5340–5347, https://doi.org/10.1021/AC990504J.

[32] S.J. Tan, W. Fang, C.T. Vangsness, B. Han, Influence of cellular microenvironment on human articular chondrocyte cell signaling, Cartilage 13 (2021) 935S–946S, https://doi.org/10.1177/1947603520941219.

[33] P.A. Levett, F.P.W. Melchels, K. Schrobback, D.W. Hutmacher, J. Malda, T.J. Klein, A biomimetic extracellular matrix for cartilage tissue engineering centered on photocurable gelatin, hyaluronic acid and chondroitin sulfate, Acta Biomater. 10 (2014) 214–223, https://doi.org/10.1016/J.ACTBIO.2013.10.005.

[34] J. Rosser, B. Bachmann, C. Jordan, I. Ribitsch, E. Haltmayer, S. Gueltekin, S. Junttila, B. Galik, A. Gyenesei, B. Haddadi, M. Harasek, M. Egerbacher, P. Ertl, F. Jenner, Microfluidic nutrient gradient-based three-dimensional chondrocyte culture-on-a-chip as an in vitro equine arthritis model, Mater Today Bio 4 (2019), https://doi.org/10.1016/J.MTBIO.2019.100023.

[35] E. Charlier, C. Deroyer, F. Ciregia, O. Malaise, S. Neuville, Z. Plener, M. Malaise, D. de Seny, Chondrocyte dedifferentiation and osteoarthritis (OA), Biochem. Pharmacol. 165 (2019) 49–65, https://doi.org/10.1016/J.BCP.2019.02.036.

[36] L.R. Zhao, R.L. Xing, P.M. Wang, N.S. Zhang, S.J. Yin, X.C. Li, L. Zhang, NLRP1 and NLRP3 inflammasomes mediate LPS/ATP-induced pyroptosis in knee osteoarthritis, Mol. Med. Rep. 17 (2018) 5463–5469, https://doi.org/10.3892/MMR.2018.8520.

[37] P. Hoff, F. Buttgereit, G.R. Burmester, M. Jakstadt, T. Gaber, K. Andreas, G. Matziolis, C. Perka, E. Rohner, E. Röhner, Osteoarthritis synovial fluid activates pro-inflammatory cytokines in primary human chondrocytes, Int. Orthop. 37 (2013) 145–151, https://doi.org/10.1007/s00264-012-1724-1.

[38] H.N. Daghestani, V.B. Kraus, Inflammatory biomarkers in osteoarthritis, Osteoarthritis Cartilage 23 (2015) 1890–1896, https://doi.org/10.1016/J.JOCA.2015.02.009.

[39] N. Miosge, M. Hartmann, C. Maelicke, R. Herken, Expression of collagen type I and type II in consecutive stages of human osteoarthritis, Histochem. Cell Biol. 122 (2004) 229–236, https://doi.org/10.1007/S00418-004-0697-6.

[40] L. Zhang, R. Xing, Z. Huang, L. Ding, L. Zhang, M. Li, X. Li, P. Wang, J. Mao, Synovial fibrosis involvement in osteoarthritis, Front. Med. 8 (2021), https://doi.org/10.3389/FMED.2021.684389.

[41] L. Troeberg, H. Nagase, Proteases involved in cartilage matrix degradation in osteoarthritis, Biochim. Biophys. Acta 1824 (2012) 133–145, https://doi.org/10.1016/J.BBAPAP.2011.06.020.

[42] Y.H. Huh, G. Lee, W.H. Song, J.T. Koh, J.H. Ryu, Crosstalk between FLS and chondrocytes is regulated by HIF-2α-mediated cytokines in arthritis, Exp. Mol. Med. 47 (2015), https://doi.org/10.1038/EMM.2015.88.

[43] M. Beekhuizen, Y.M. Bastiaansen-Jenniskens, W. Koevoet, D.B.F. Saris, W.J. A. Dhert, L.B. Creemers, G.J.V.M. Van Osch, Osteoarthritic synovial tissue inhibition of proteoglycan production in human osteoarthritic knee cartilage: establishment and characterization of a long-term cartilage-synovium coculture, Arthritis Rheum. 63 (2011) 1918–1927, https://doi.org/10.1002/ART.30364.

[44] A.I. Caplan, D. Correa, The MSC: an injury drugstore, Cell Stem Cell 9 (2011) 11–15, https://doi.org/10.1016/j.stem.2011.06.008.

[45] U. Anil, D.H. Markus, E.T. Hurley, A.K. Manjunath, M.J. Alaia, K.A. Campbell, L. M. Jazrawi, E.J. Strauss, The efficacy of intra-articular injections in the treatment of knee osteoarthritis: a network meta-analysis of randomized controlled trials, Knee 32 (2021) 173–182, https://doi.org/10.1016/J.KNEE.2021.08.008.

[46] A.I. Tsuchida, M. Beekhuizen, M.C. t Hart, T.R.D.J. Radstake, W.J.A. Dhert, D.B. F. Saris, G.J.V.M. Van Osch, L.B. Creemers, Cytokine profiles in the joint depend on pathology, but are different between synovial fluid, cartilage tissue and cultured chondrocytes, Arthritis Res. Ther. 16 (2014), https://doi.org/10.1186/S13075-014-0441-0.

[47] A. Gómez-Aristizábal, A. Sharma, M.A. Bakooshli, M. Kapoor, P.M. Gilbert, S. Viswanathan, R. Gandhi, Stage-specific differences in secretory profile of mesenchymal stromal cells (MSCs) subjected to early- vs late-stage OA synovial fluid, Osteoarthritis Cartilage 25 (2017) 737–741, https://doi.org/10.1016/J.JOCA.2016.11.010.

[48] C. Manferdini, M. Maumus, E. Gabusi, A. Piacentini, G. Filardo, J.A. Peyrafitte, C. Jorgensen, P. Bourin, S. Fleury-Cappellesso, A. Facchini, D. Noël, G. Lisignoli, Adipose-derived mesenchymal stem cells exert antiinflammatory effects on chondrocytes and synoviocytes from osteoarthritis patients through prostaglandin E2, Arthritis Rheum. 65 (2013) 1271–1281, https://doi.org/10.1002/ART.37908.

[49] G.M. van Buul, E. Villafuertes, P.K. Bos, J.H. Waarsing, N. Kops, R. Narcisi, H. Weinans, J.A.N. Verhaar, M.R. Bernsen, G.J.V.M. van Osch, Mesenchymal stem cells secrete factors that inhibit inflammatory processes in short-term osteoarthritic synovium and cartilage explant culture, Osteoarthritis Cartilage 20 (2012) 1186–1196, https://doi.org/10.1016/J.JOCA.2012.06.003.

[50] L. Bian, D.Y. Zhai, R.L. Mauck, J.A. Burdick, Coculture of human mesenchymal stem cells and articular chondrocytes reduces hypertrophy and enhances functional properties of engineered cartilage, Tissue Eng Part A 17 (2011) 1137–1145, https://doi.org/10.1089/TEN.TEA.2010.0531.

[51] J.M. Milner, A.D. Rowan, T.E. Cawston, D.A. Young, Metalloproteinase and inhibitor expression profiling of resorbing cartilage reveals pro-collagenase activation as a critical step for collagenolysis, Arthritis Res. Ther. 8 (2006), https://doi.org/10.1186/ar2034.

[52] Q. Hu, M.E.-I. journal of molecular sciences, Undefined 2021, overview of MMP-13 as a promising target for the treatment of osteoarthritis, Mdpi.ComQ Hu, M EckerInternational Journal of Molecular Sciences, 2021•mdpi.Com (2021), https://doi.org/10.3390/ijms22041742.

[53] S. Fuchs, A. Skwara, M. Bloch, B. Dankbar, Differential induction and regulation of matrix metalloproteinases in osteoarthritic tissue and fluid synovial fibroblasts,

Osteoarthritis Cartilage 12 (2004) 409–418, https://doi.org/10.1016/j.joca.2004.02.005.
[54] P.S. Burrage, Matrix metalloproteinases: role in arthritis, Front. Biosci. 11 (2006) 529, https://doi.org/10.2741/1817.
[55] S. Bersini, C. Arrigoni, G. Talò, C. Candrian, M. Moretti, Complex or not too complex? One size does not fit all in next generation microphysiological systems, iScience 27 (2024), https://doi.org/10.1016/J.ISCI.2024.109199.